Nicotinamide N-methyltransferase in endothelium protects against oxidant stress-induced endothelial injury

(Article begins on next page)

27 July 2025

Title

Nicotinamide N-methyltransferase in endothelium protects against oxidant stress-induced endothelial injury

Authors

Roberto Campagna[a,b], Łukasz Mateuszuk[b], Kamila Wojnar-Lason[b,c], Patrycja Kaczara[b], Anna Tworzydło[b], Agnieszka Kij[b], Robert Bujok[d], Jacek Mlynarski[d], Yu Wang[e], Davide Sartini[a], Monica Emanuelli[a#], Stefan Chlopicki[b,c#].

Affiliations:
[a] Department of Clinical Sciences, Polytechnic University of Marche, Ancona, Italy.
[b] Jagiellonian Centre for Experimental Therapeutics (JCET), Jagiellonian University, Krakow, Poland.
[c] Jagiellonian University Medical College, Faculty of Medicine, Chair of Pharmacology, Krakow, Poland.
[d] Institute of Organic Chemistry, Polish Academy of Sciences, Warsaw, Poland.
[e] State Key Laboratory of Pharmaceutical Biotechnology and Department of Pharmacology and Pharmacy, Li Ka Shing Faculty of Medicine, The University of Hong Kong, LKS Faculty of Medicine Building, 21 Sassoon Road, Pokfulam, Hong Kong, China.

[#] Corresponding authors

Abstract

Nicotinamide N-methyltransferase (NNMT, EC 2.1.1.1.) plays an important role in the growth of many different tumours and is also involved in various non-neoplastic disorders. However, the presence and role of NNMT in the endothelium has yet to be specifically explored. Here, we characterized the functional activity of NNMT in the endothelium and tested whether NNMT regulates endothelial cell viability. NNMT in endothelial cells (HAEC, HMEC-1 and EA.hy926) was inhibited using two approaches: pharmacological inhibition of the enzyme by NNMT inhibitors (5-amino-1-methylquinoline – 5MQ and 6-methoxynicotinamide – JBSF-88) or by shRNA-mediated silencing. Functional inhibition of NNMT was confirmed by LC/MS/MS-based analysis of impaired MNA production. The effects of NNMT inhibition on cellular viability were analyzed in both the absence and presence of menadione.

Our results revealed that all studied endothelial lines express relatively high levels of functionally active NNMT compared with cancer cells (MDA-MB-231). Although the aldehyde oxidase 1 enzyme was also expressed in the endothelium, the further metabolites of N1-methylnicotinamide (N1-methyl-2-pyridone-5-carboxamide and N1-methyl-4-pyridone-3-carboxamide) generated by this enzyme were not detected, suggesting that endothelial NNMT-derived MNA was not subsequently metabolized in the endothelium by aldehyde oxidase 1. Menadione induced a concentration-dependent decrease in endothelial viability as evidenced by a decrease in cell number that was associated with the upregulation of NNMT and SIRT1 expression in the nucleus in viable cells. The suppression of the NNMT activity either by NNMT inhibitors or shRNA-based silencing significantly decreased the endothelial cell viability in response to menadione. Furthermore, NNMT inhibition resulted in nuclear SIRT1 expression downregulation and upregulation of the phosphorylated form of SIRT1 on Ser47. In conclusion, our results suggest that the endothelial nuclear NNMT/SIRT1 pathway exerts a cytoprotective role that safeguards endothelial cell viability under oxidant stress insult.

Keywords

Nicotinamide N-methyltransferase, NNMT, endothelium, oxidative stress.

Abbreviations

Nicotinamide N-methyltransferase (NNMT), 5-amino-1-methylquinoline (5MQ), 6-methoxynicotinamide (JBSF-88), aldehyde oxidase 1 (AOX1), N1-methyl-2-pyridone-5-carboxamide (Met2py), N1-methyl-4-pyridone-3-carboxamide (Met4py), nicotinamide (NAM), nicotinamide adenine dinucleotide (NAD+), S-adenosyl-L-homocysteine (SAH), 1-methylnicotinamide (MNA), oral squamous cell carcinoma (OSCC), renal clear cell carcinoma (ccRCC), cyclooxygenase-2 (COX-2), prostacyclin (PGI2), nitric oxide (NO), confocal quantitative image cytometer (CQ1), mitochondrial stress test (MST), peroxisome proliferator-activated receptor-g coactivator-1a (PGC-1a), forkhead transcription factor O (FoxO), nuclear factor kB (NFkB), endothelial nitric oxide synthase (eNOS), notch1 intracellular domain (NICD), liver kinase B1 (LKB1), tumour suppressor protein 53 (p53), cyclin-dependent kinase 5 (CDK5).

1. Introduction

Nicotinamide-N-methyltransferase (NNMT) (E.C. 2.1.1.1) catalyzes the N-methylation of nicotinamide (NAM) and structurally related compounds utilizing S-Adenosyl methionine (SAM) as the methyl donor to produce S-adenosyl-L-homocysteine (SAH) and 1-methylnicotinamide (MNA). MNA is further oxidized by aldehyde oxidase 1 (AOX1) into two related compounds, N1-methyl-2-pyridone-5-carboxamide (Met2py) and N1-methyl-4-pyridone-3-carboxamide (Met4py) [1,2]. Nicotinamide (NAM) is a key precursor for the synthesis of nicotinamide adenine dinucleotide (NAD+) and, therefore, NNMT activity is linked to the metabolism of NAD+, which is a master regulator of energy metabolism and influences cell life span [3,4]. NNMT is predominantly expressed in the liver but was also detected in other tissues, including the kidney, heart, lung, brain, placenta, striated muscle tissue and adipose tissue [1,5,6]. The role of the NNMT/MNA metabolic pathway seems to be distinct in various organs and cells and was most studied in the liver, adipose tissue as well as in cancer cells.

In the liver, NNMT expression regulates serum cholesterol and triglycerides, and this effect was attributed to MNA, which enhances SIRT1 protein levels and activity [7]. The cytoprotective role of NNMT against oxidative injury and endoplasmic reticulum stress, induced by iron overload, was also reported [8]. On the other hand, it was found that transgenic mice that overexpress NNMT displayed fatty livers and fibrosis, particularly after NAM supplementation [9]. Furthermore, increased circulating MNA levels positively correlated with obesity and diabetes [10,11] and in a recent study, NNMT inhibitor (JBSF-88) reduced body weight, improved insulin sensitivity and normalized glucose tolerance in mice fed a high-fat diet [12]. Similarly, another NNMT inhibitor, 5-amino-1-methylquinoline (5MQ), was shown to reverse high-fat diet-induced obesity in mice [13]. As in human adipose tissue, the NNMT expression positively correlates with adiposity and insulin resistance, and the effects of NNMT inhibition *in vivo* preventing fat accumulation and improving glucose tolerance in C57BL6 mice (fed a high-fat diet) might be related to the inhibition of NNMT in adipose tissue not in the liver [10,14,15].

Numerous reports have described the pathophysiological role of upregulated NNMT in various types of solid tumours, including oral squamous cell carcinoma (OSCC) [16], papillary thyroid cancer [17], lung cancer [18], gastric cancer [19], pancreatic cancer [20], colorectal cancer [21], renal clear cell carcinoma (ccRCC) [22,23], bladder cancer [24], ovarian clear cell carcinoma [25], cutaneous and oral malignant melanoma [26,27]. NNMT overexpression has been linked to increased tumorigenicity and poor prognosis. NNMT knockdown inhibited the proliferation and/or metastasis in ccRCC, pancreatic cancer cell Panc-1, OSCC and other cancers [28–30]. Although several studies have confirmed the functional pro-tumorigenic role of NNMT in these tumours, the mechanisms involved were not fully elucidated. Recently, Ulanovskaya et al. suggested that NNMT may act as a methyl donor sink because SAM is a co-substrate required by all methyltransferases, including NNMT and histone methyltransferases [31].

Alterations in NNMT expression and activity were found to be upregulated not only in cancer but also in several non-neoplastic disorders, including Parkinson's disease [32,33], metabolic syndrome [34] chronic obstructive pulmonary disease [35] and pulmonary hypertension [36]. However, it is still not clear whether the upregulated NNMT/MNA pathway in these diseases contributes to the pathology or represents a compensatory mechanism [37,38].

Both positive and detrimental roles of endogenous NNMT enzyme activity, depending on the experimental model and tissue studied, have been suggested. However, exogenous MNA has been repeatedly shown to afford vasoprotective pharmacological activities. For instance, MNA displayed anti-thrombotic activity in rats with arterial thrombosis through a mechanism involving cyclooxygenase-2 (COX-2) and prostacyclin (PGI2) [39]. Accordingly, MNA could be regarded as the first class of molecule to boost the endogenous COX-2/PGI2 pathway. Several beneficial effects of exogenous MNA have been reported, including PGI2-mediated anti-inflammatory [40], gastroprotective [41], hepatoprotective [42,43],

neuroprotective [44,45] as well as anti-metastatic effects [46,47]. Furthermore, the anti-atherosclerotic activity of MNA [48] was associated with an improvement in PGI2- and nitric oxide (NO)-dependent endothelial function, the latter effect confirmed also using functional 3D MRI-based assessment of endothelial function *in vivo* [49].

Taken together, exogenous MNA positively modulates endothelial and vascular function, but it is still not known whether the functional NNMT is present in endothelial cells and whether endothelial NNMT activity modulates endothelial response to injury. Therefore, the aim of this work was to determine whether endothelial cells display an active NNMT/AOX1 pathway and whether NNMT inhibition modulates cell viability in response to oxidative stress.

2. Materials and methods

2.1 Cell culture

The human endothelial cell line EA.hy926, purchased from the American Type Culture Collection (ATCC, Rockville, MD, USA), was cultured in DMEM high-glucose medium (4.5 g/l), supplemented with 10% foetal bovine serum (FBS), glutamine 2 mM and gentamicin 50 μg/ml. The human aortic endothelial cell line (HAEC) and the human microvascular endothelial cell line (hLMVEC) were purchased from Lonza (Basel, Switzerland) and were cultured in a 2% FBS endothelial growth medium (EGM)-2 Bullet Kit (Lonza), according to the manufacturer's instructions, with the addition of 50 μg/ml of gentamicin.

All experiments were performed using HAECs between the 2nd and 5th passages. The human microvascular endothelium cell line HMEC-1, purchased from the ATCC, was cultured in MCDB131 medium (Gibco) supplemented with 10% FBS, 10 mM glutamine, 1 μg/ml hydrocortisone and 10 ng/ml epidermal growth factor (EGF). All cells were grown at 37 °C in a humidified 5% CO_2 incubator.

2.2 Assessment of NNMT and AOX1 expression in endothelium by western blotting

Samples containing 50 μg protein were subjected to sodium dodecyl sulphate-polyacrylamide gel electrophoresis (SDS-PAGE) using a running gel of 12% polyacrylamide. Proteins were transferred to polyvinylidene fluoride (PVDF) membranes at 0.08 mA overnight, using a wet transfer method. PVDF membranes were blocked overnight at 4 °C in 1X phosphate-buffered saline (PBS) solution containing 5% non-fat dry milk and 0.05% tween-20. After washing three times with 1X PBS containing 0.05% tween-20, the membranes were incubated with rabbit polyclonal antibody against NNMT (Sigma-Aldrich, St. Louis, MO, USA) or AOX1 (Thermo Fisher Scientific, Waltham, MA, USA) (1:1000 dilution) for 2 h, followed by incubation with horseradish peroxidase (HRP)-conjugated goat anti-rabbit IgG (Thermo Fisher Scientific) (1:2000 dilution) for 1 hour. Protein signals were visualized using an enhanced SuperSignal West Femto Maximum Sensitivity Substrate (Thermo Fisher Scientific). The chemiluminescent signal of NNMT protein detected in blots was acquired using a ChemiDoc XRS + System (Bio-Rad Laboratories).

2.3 Assessment of NNMT activity by LC/MS/MS based-MNA measurements

Cells were seeded in 24-well plates to have 90% confluence on the day of the experiment. After 24 h, the medium was removed, and cells were washed twice by PBS 1X. Cells were then incubated with 500 μl Krebs buffer for 4 h at 37 °C. Krebs buffer was then replaced with 300 μl of fresh buffer with nicotinamide 100 μM and SAM 10μM. To measure NNMT activity in the liver, male 12–16-week-old C57Bl/6J mice were used (Jackson Laboratories, Bar Harbor, ME, USA). Mice were housed in colony cages in a temperature-controlled environment (22–25°C) with a 12-hour light/dark cycle and had free access to food and water. Mice were anesthetized with ketamine (100 mg/kg) and xylazine (10 mg/kg) administered intraperitoneally, and mice livers were perfused by PBS 1X and used for *ex vivo* studies. Mice liver aliquots (20 mg) were incubated in Krebs buffer for 1 h at 37 °C.

At fixed time-points, 50 μl of extracellular fluid taken from endothelial cells or liver pieces were collected, and in each sample, the MNA concentration was analyzed by LC/MS/MS as described previously [36,48]. Briefly, an aliquot of 50 μl of extracellular fluid was spiked with 5 μL of internal standard (deuterated analogues of analytes) at a concentration of 25 μg/ml. Samples were subjected to deproteinization with 100 μL of acidified acetonitrile (0.1% formic acid), vortexed, cooled at 4 °C for 15 min and centrifuged (15000 x g, 15 min, 4 °C). Supernatants were injected into an LC column. Chromatographic analysis was performed using an UltiMate 3000 LC system (Thermo Scientific Dionex, Sunnyvale, CA) consisting of a pump (DGP 3600RS), column compartment (TCC 3000RS), autosampler (WPS-3000TRS) and SRD-3600 solvent rack (degasser). Chromatographic separation was carried out on an Aquasil C18 analytical column (4.6 mm x 150 mm, 5 mm; Thermo Scientific). The mobile phase consisted of acetonitrile (A) and 5 mM ammonium formate (B) in isocratic elution (80:20 v/v) at a flow rate of 0.8 ml/min.

Detection was performed using a TSQ Quantum Ultra mass spectrometer equipped with a heated electrospray ionization interface (HESI-II Probe) (Thermo Scientific, Waltham, MA, US). The mass spectrometer was operating in the positive ionization using selected reactions monitoring mode (SRM), monitoring the transition of the protonated molecular ions m/z 153–110 for Met2PY, m/z 156 → 113 for Met2PY-d3, m/z 153–136 for Met4PY, m/z 156 → 139 for Met4PY-d3, m/z 123–80 for NA, m/z 127-84 for NA-d4 and m/z 137–94 for MNA, m/z 140 → 97 for MNA-d3. Data acquisition and processing were accomplished using Xcalibur 2.1 software.

The following reagents were used as measurement standards: NAM and MNA obtained from Sigma-Aldrich and N-methyl-4- pyridone-3-carboxamide (Met-2PY) and N-methyl-2-pyridone-5- carboxamide (Met-4PY) purchased from TLC PharmaChem (Vaughan, ON, Canada). Deuterated analytes were used as internal standards. NA-d4 and NAM-d4 were purchased from Sigma-Aldrich and Dr. Ehrenstorfer GmbH (Augsburg, Germany), respectively. Met2PY-d3 and Met-4PY-d3 were obtained from TLC PharmaChem, and MNA-d3 was synthesized by Dr. Adamus (Technical University, Lodz, Poland). LCMS–grade acetonitrile, ammonium formate and formic acid were purchased from Sigma-Aldrich. Ultrapure water was obtained from a Millipore system (Direct-Q 3UV).

## 2.4 Synthesis of NNMT inhibitors

6-Methoxy-3-pyridinecarboxamide (JBSF-88, compound **3**) was synthesized from commercially available 2-chloro-5-cyanopyridine (**1**) according to the following scheme:
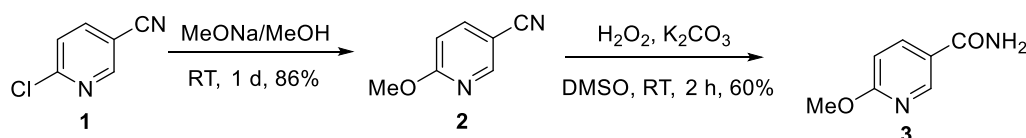
5-Cyano-2-methoxypyridine **2** was prepared by substitution of chlorine with methoxide anion in MeOH according to a slightly modified literature protocol [50]. 6-Methyoxy-3-pyridinecarboxamide **3** was synthesized from compound **2** in a reaction with H_2O_2 in the presence of solid K_2CO_3 in DMSO [51].

K_2CO_3 (0.332 g, 2.40 mmol) was added to a solution of 5-cyano-2-methoxypyridine **2** (0.648 g, 4.75 mmol) in DMSO (15 mL). The mixture was cooled to 10 °C, and 30% H_2O_2 (4.8 mL) was added after 5 min, maintaining the temperature below 35 °C. When the addition was completed, the suspension was stirred at RT for 2 h. The mixture was poured into water (20 mL), extracted with AcOEt (5 × 20 mL), and the combined extracts were washed with water (3 × 20 mL), dried and evaporated. The crude product was washed with $CHCl_3$ (3 × 5 mL) to give 0.435 g (60%) of amide **3** as a white solid. ^1H NMR (500 MHz, CDCl$_3$): δ 8.68 (d, J=2.4 Hz, 1H), 8.13 (dd, J=8.7, 2.4 Hz, 1H), 7.96 (bs, 1H), 7.37 (bs, 1H), 6.87 (d, J=8.7 Hz, 1H), 3.91 (s, 3H). ^{13}C NMR (125 MHz, CDCl$_3$): δ 166.1, 165.1, 147.3, 138.3, 123.5, 110.0, 53.5. HRMS–ESI$^+$ (m/z, MeOH): calcd for $C_7H_9N_2O_2$ [M+H]$^+$, 153.0664; found: 153.0660. Calcd for $C_7H_9N_2O_2$ %C, 55.26;%H, 5.30,%N, 18.60, found %C, 55.24;%H, 5.11,%N, 18.16.

5-Amino-1-methylquinolinium iodide (5MQ, compound **5**) was obtained from commercially available 5-amino-quinoline **4** according to an improved literature protocol [52].
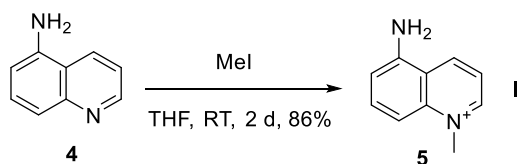
Iodomethane (0.160 mL, 0.365 g, 2.6 mmol) was added to a solution of 5-aminoquinoline **4** (0.277 g, 1.9 mmol) in THF (7 mL) and the solution was stirred at RT for 1 d when red solid precipitated. The product

was filtered-off, washed with THF (2 × 5 mL) and dried in a vacuum to give 0.240 g of compound **5**. The filtrate was evaporated, the residue was dissolved in THF (4 mL), iodomethane (0.090 mL) was added, and the mixture was stirred at RT for another day. Product was filtered-off, washed with THF and dried to give 0.228 g (86%) of **5**. ^{1}H NMR data were identical to that previously published [52].

2.5 NNMT gene silencing and stable cell strain selection

Cells grown to 80–90% confluence were removed from the T25 flask using 0.025% trypsin/EDTA (Gibco) at room temperature. $2x10^6$ cells were resuspended in Optimem (Gibco) + 10% FBS. Twenty µg of shRNA plasmids against NNMT (pLKO.1-330, 1-448 and 1-711) or of empty pLKO.1 puro (pLKO.1 Ø) vector (Sigma-Aldrich, St. Luis, MO) were mixed with the cell suspension to a final volume of 400 µl and incubated for 10 min at +4 °C. Control EA.hy926 cells (mock) were treated with transfection reagents only.

The cell suspension was placed in a 4 mm-gap electroporation cuvette (BTX) and electroporated at capacitances of 900 µF in combination with 200 V.

The electroporated cells were left in the cuvette for 10 min at room temperature and then transferred in T75 flasks with complete growth medium. Forty-eight hours after transfection, clones stably downregulating NNMT were selected by maintaining cells in complete medium containing puromycin (0.4 µg/ml), with medium changes every 48 h. All subsequent experiments involving these clones were performed by growing cells in complete medium containing puromycin.

2.6 Determination of NNMT silencing by real time-PCR

Total RNA was isolated through the SV Total RNA Isolation System (Promega, Madison, WI, USA), according to the manufacturer's protocol. Total RNA (2 µg) was reverse-transcribed in a total volume of 25 µl for 60 minutes at 37 °C with M-MLV Reverse Transcriptase (Promega, Madison, WI, USA), using random primers. cDNA samples were used to perform subsequent real-time PCR analysis. To evaluate NNMT mRNA expression quantitatively, a real-time PCR assay was performed using a CFX96 Real-Time PCR Detection System (Bio-Rad Laboratories, Hercules, CA, USA). cDNA, generated as described above, was used as a template. The primers used were 5′-GAA TCA GGC TTC ACC TCC AA-3′ (forward) and 5′-TCA CAC CGT CTA GGC AGA AT-3′ (reverse) for NNMT, and 5′-TCC TTC CTG GGC ATG GAG T-3′ and 5′-AGC ACT GTG TTG GCG TAC AG-3′ for β-actin.

Both genes were run in duplicate for 40 cycles at 94 °C for 30 seconds and 58 °C for 30 seconds, using a SsoFast EvaGreen Supermix (Bio-Rad Laboratories, Hercules, CA, USA). All samples were tested in triplicate using the β-actin gene for data normalization. Direct detection of PCR products was monitored by measuring the fluorescence produced by EvaGreen dye binding to double-stranded DNA after every cycle. These measurements were then plotted against cycle numbers. The parameter threshold cycle (Ct) was defined as the cycle number at which the first detectable increase above the threshold in fluorescence was observed. Following NNMT gene silencing in EA.hy926 cells, fold changes in relative gene expression were calculated by $2^{-\Delta(\Delta Ct)}$, where $\Delta Ct = Ct (NNMT) - Ct (\beta\text{-actin})$ and $\Delta(\Delta Ct) = \Delta Ct$ (cells transfected with plasmid vectors) - ΔCt (mock).

2.7 Cell viability assay in menadione-induced endothelial cell injury

To assess cell viability, cells were cultivated in full medium and treated with menadione (Sigma Aldrich, Saint Louis, MO, USA) for 24, 48 or 72h and 5MQ or JBSF-88 when indicated. Additionally, cells were treated with specific SIRT1 inhibitor EX-527 (Sigma Aldrich, Saint Louis, MO, USA) to examine the role of sirtuin-dependent pathways in menadione-induced endothelial injury. (Cells were washed with PBS before fixing (with a solution of 4% paraformaldehyde at room temperature) or before live cell imaging and incubated with a solution of YO-PRO™-1 Iodide (Thermo Fisher Scientific, USA) diluted 1:1000 in the dark, at 37 °C for 30 min. For nuclei counterstaining, a Hoechst 33258 solution (Sigma Aldrich, Saint Louis, MO, USA) was used. Imaging was performed with a confocal quantitative image cytometer (CQ1)

(Yokogawa, Musashino, Tokyo, Japan). Images were analyzed via Columbus 2.4.2 software (Perkin Elmer, Waltham, MA, USA) and the number of cells and/or number of cells positive to the YO-PRO™-1 iodide stain was calculated. Both NNMT inhibitors were tested for toxicity by MTT assay and they did not affect the cell viability in a statistically significant way for all the concentrations and time-points used in this study.

2.8 Expression of SIRT1, pSIRT1, p53, acetyl-p53 and NNMT by immunocytochemistry

Cells were plated in 96-well format on black Corning multiplates with a clear bottom. After the treatment, cells were fixed with a 4% formalin solution for 10 min, washed with PBS and then incubated with a blocking solution containing 5% normal goat serum (Sanquin, Amsterdam, Netherlands) to minimalize non-specific binding of antibodies. For indirect immunohistochemical detection, cells were incubated overnight with the following primary antibodies: NNMT polyclonal antibody, p53 monoclonal antibody, Acetyl(Lys382)p53 monoclonal antibody (Thermo Fisher Scientific, Waltham, MA, USA), SIRT1 monoclonal antibody (Merck Millipore, Burlington, MA, USA), Phospho-SIRT1 (Ser47) polyclonal antibody (Cell Signaling Technology, USA). Secondary antibodies used were Alexa Fluor 647-conjugated goat anti-rabbit and Cy3-conjugated goat-anti-mouse (Jackson Immuno, Cambridgeshire, UK). For nuclei counterstaining, Hoechst 33258 solution was used. Images of immunostained cells were taken using a CQ1 (Yokogawa, Musashino, Tokyo, Japan) and CQ 1.04 software, then analyzed automatically with Columbus 2.4.2 software (Perkin Elmer, Waltham, MA, USA). For data normalization, each immunostaining (n=6) was performed using cells with similar confluence (≥90%), the same primary and secondary antibody concentration and constant incubation time for each staining step. As a negative control, cells treated only with secondary antibodies were used to estimate the background signal.

2.9 Cell proliferation assay using electric cell-substrate impedance sensing

Cells were grown on the surface of planar golden electrodes of an electric cell-substrate impedance sensing set-up (ECIS), and the resistance of the cell-covered electrode was measured continuously at a frequency of 4,000 Hz. Because of the insulating properties of cell membranes, the resistance increases with increasing coverage of the electrode. HAECs and HMEC-1 cells were seeded in 96-well, gold-film electrode-coated 96W1E+PET arrays (Applied Biophysics). The resistance parameter was constantly monitored up to 125 h after seeding.

2.10 Mitochondrial stress test

For the mitochondrial stress test (MST), HAEC cells were seeded into Seahorse XFe 96-well plates at a density of 1.5×10^3 per well to produce confluency on the next day. The cells were treated with JBSF or 5MQ or not treated for 72 h, and the medium was exchanged after 24 and 48 h before MST. An assay medium for MST was prepared on the day of the experiment by supplementation of Seahorse DMEM XF Base medium (Agilent) with glucose (1 g/l; Merck), glutamine (2 mM; Sigma-Aldrich) and sodium pyruvate (1 mM; Sigma-Aldrich) and adjusting the pH to 7.4 using 0.1 M NaOH (Sigma-Aldrich). Immediately prior to MST, the cells were washed twice with the assay medium, then fresh assay medium was added and cells were incubated for 1 h at 37 °C without CO_2. Changes in oxygen consumption rate (OCR) and extracellular acidification rate (ECAR) were recorded over time. After four basal measurements, oligomycin (1 µg/ml; Calbiochem) was added from port A, followed by three measurements, then FCCP (1.5 µM; Sigma-Aldrich) was added from port B, followed by three measurements, and finally, rotenone (0.5 µM; Sigma-Aldrich) with antimycine A (0.5 µM; Sigma-Aldrich) were added from port C, followed by three measurements. Concentrations of oligomycin, FCCP, rotenone and antimycine A had been optimized in preliminary experiments. After the assay, cells were washed once with DPBS (Gibco), 10 µl of 0.1% Triton X-100 (Sigma-Aldrich) in DPBS was added per well, and cells were frozen at -80 °C. On the next day, the protein content was measured using a Bicinchoninic Acid Protein Determination Kit (Sigma-Aldrich). The data were normalized for protein content and analyzed using the Seahorse XF Cell Mito Stress Test Report Generator

(Agilent). The following parameters of mitochondrial function were analyzed: basal respiration, proton leakage, ATP production, maximal respiration, spare respiratory capacity and non-mitochondrial oxygen consumption.

2.11 Statistical analysis

Data were analyzed using GraphPad Prism software version 6.00 for Windows (GraphPad Prism Software, San Diego, CA, USA). Differences between groups were determined using the Mann-Whitney nonparametric test, or Kruskal-Wallis one-way ANOVA, followed by a post-hoc Dunn test. A p-value < 0.05 was considered statistically significant.

3. Results

3.1 NNMT expression in endothelial cells

As shown in Fig. 1, endothelial cells expressed NNMT, but the level of expression was not uniform for all endothelial cells tested. Surprisingly, NNMT expression in HAECs was comparable to the expression of NNMT in human MDA-MB-231 breast cancer cells. With the exception of EA.hy926, in other types of endothelial cells (HMECs-1, HUVECs and hLMVECs), the expression of NNMT was higher as compared with HAECs (by approximately 4.0, 6.4 and 1.8 folds, respectively). NNMT protein was not detected in MCF-7 cells, used here as a negative control.

In contrast to the different expression of NNMT in various endothelial cells lines, the expression level of AOX1 was comparable for tested endothelial cells (HAEC, HMEC-1, HUVEC, hLMVEC EA.hy926) was approximately two folds lower than in MDA-MB-231 breast cancer cells (Figure 1B).

3.2 Pharmacological inhibition of NNMT in endothelial cells

Both NNMT inhibitors, 5-Amino-1-methylquinoline (5MQ) and 6-methoxynicotinamide (JBSF-88) incubated for 1 hour inhibited NNMT activity in a concentration-dependent manner in HMEC-1 (Fig. 2A) and HAECs (Fig. 2B), as evidenced by a progressive, concentration-dependent decrease in MNA production. In HMEC-1, the efficiency of inhibition was slightly higher for 5MQ as compared with JBSF-88, but both inhibitors at a concentration of 30 μM profoundly inhibited NNMT activity and decreased MNA production by >90% and >70%, respectively (Fig. 2A). Similarly, in HAECs, both inhibitors at a concentration of 30 μM lowered MNA by >90% (Fig. 2B). Longer incubation with inhibitors (24 h incubation) in HMEC-1 also resulted in a profound inhibition of NNMT activity (by 75.90% and 59.79% for 30 μM concentration of 5MQ and JBSF-88, respectively) (Fig. 2C).

A similar degree of NNMT inhibition by 5MQ and JBSF-88 was achieved in the liver because a 30 μM concentration of the 5MQ or JBSF-88 inhibited NNMT by >90% (Fig. 2D).

3.3 Effect of NNMT inhibition on endothelial cell viability in response to menadione-induced oxidative stress

To examine the effects of NNMT inhibition on endothelial response to oxidative stress, HAEC and HMEC-1 cells were incubated with increasing concentrations of menadione in the absence or presence of NNMT inhibitors (5MQ or JBSF-88). Both inhibitors were given at a concentration of 30 μM, inhibiting NNMT activity >90% (Fig. 2). As shown in Figure 3, in the presence of NNMT inhibitors, menadione significantly decreased the cell viability as compared to the cells treated with menadione alone. A similar pattern of potentiated menadione-induced injury by NNMT inhibition was observed in HAEC (Fig. 3A, B) and HMEC-1 (Fig. 3C, D) cells.

To confirm that the observed reduction in cell viability was a consequence of the NNMT inhibition and not a non-specific effect, the same experiment was performed on EA.hy926 cell lines in which the NNMT was efficiently silenced by shRNAs (Fig. 4A, B). NNMT-silenced endothelial cell lines displayed a marked reduction in cell viability in response to menadione as compared to the empty plasmid-transfected control, thus confirming that NNMT exerts a protective role in the endothelium against oxidative stress (Fig. 4C).

In the presence of the NNMT inhibitor JBSF-88, low concentrations of menadione triggered a moderate but significant increase in the percentage of Yo-Pro1 iodide-positive cells (Fig. 5A). Interestingly, when HAECs were incubated with NNMT inhibitors alone for a longer time period of 72 h (5MQ or JBSF-88 3-50μM), there was a clear concentration-dependent increase in Yo-Pro1 iodide-positive cells from approximately 4.05% to 8–10% (Fig. 5B, C), suggesting that NNMT inhibition alone affects plasma membrane integrity.

3.4 NNMT inhibition does not affect the proliferation rate nor the bioenergetics of endothelial cells

To determine whether the effects of NNMT inhibition on cell viability are related to the effects on endothelial cell proliferation or to endothelial bioenergetics, we analyzed how 5MQ and JBSF-88 affected cell proliferation (ECIS assay) and mitochondrial respiration (Seahorse XF96 Analyzer). As shown in Fig. 6, the long-term NNMT inhibition by JBSF-88 did not affect the proliferation of HAEC or HMEC-1 cells (Fig. 6E, F) and did not significantly affect mitochondrial function (Fig. 6A-D) as evidenced by unchanged basal and maximal mitochondrial respiration as well as other measured parameters (not shown).

3.5 NNMT inhibition alters nuclear pSIRT1/SIRT1 expression ratio in menadione-induced oxidant stress

As shown in Fig. 7, inhibition of NNMT by 5MQ or JBSF-88 resulted in a significant downregulation of nuclear SIRT1 expression, whereas phosphorylation of nuclear SIRT1 at S47 was significantly elevated (Fig. 7). Noticeably, the ratio pSIRT1/SIRT1 increased in NNMT-inhibited endothelial cells as compared to control cells (Fig. 7). Altogether, these results revealed that NNMT inhibition triggered a decrease in nuclear SIRT1 expression associated with an increase of nuclear SIRT1 phosphorylation at S47 in endothelial cells. Menadione alone induced a parallel increase in the nuclear expression of SIRT1 enzyme, together with its phosphorylated form at Ser47 (pSIRT1) (Fig. 8). Inhibition of SIRT1 by EX-527 potentiated the effect of menadione on cellular viability (Fig.9A) and increased menadione-induced expression of p53 in HAEC cells (Fig. 9B), while the combination of menadione and EX-527 had no effect on the expression of acetylated p53 (Fig. 9C). Menadione-induced endothelial cell injury was associated with NNMT enzyme expression upregulation as evidenced by immunocytochemistry (Fig. 8), and an inverse correlation was found between cell viability and NNMT expression, (Fig. 8A, B) suggesting that increased activity of NNMT in menadione-treated cells represents a compensatory response to menadione-induced oxidant stress response.

4. Discussion

Despite the abundant literature regarding the role of nicotinamide N-methyltransferase (NNMT) activity in various physiological and pathophysiological conditions, up to now, the presence and functional role of NNMT in the endothelial cells had not been characterized. In this work, we demonstrated to our knowledge, for the first time, that endothelial cells display a relatively high expression and activity of NNMT that safeguards endothelial cell viability against oxidative stress-induced insult.

We demonstrated that endothelial cells exhibited an NNMT activity that was comparable to the activity of this enzyme in the liver, the organ with high NNMT expression, and comparable or even higher expression than in a breast cancer cell line, the phenotype of which is known to be dependent on NNMT activity [53]. On the other hand, although endothelial cells expressed AOX1 at the protein level, the further metabolites of MNA (Met2Py and Met4Py) were not detected either in HAEC or in HMEC-1, suggesting that endothelial NNMT-derived MNA is not further metabolized by AOX1 in the endothelium or that this metabolism is negligible in our experimental setting. The latter enzyme most likely metabolizes other substrates in the endothelium [54]. Remarkably, in all our assays, the MNA concentration was detected in the extracellular fluid, suggesting that extracellular endothelial-derived MNA could have a biological role [39,55,56] and could contribute to altered MNA plasma concentration in various diseases [10] and conditions [57].

In the present work, the functional role of NNMT in endothelial cells was analyzed using two NNMT inhibitors; 5-amino-1-methylquinoline (5MQ) and 6-methoxynicotinamide (JBSF-88) [12,52] and shRNA-mediated silencing. In our hands, both inhibitors profoundly inhibited NNMT activity at 10–30 μM concentration in HMEC-1 and in HAECs with a similar level of inhibition as in the liver tissue, supporting the validity of a pharmacological approach to inhibit NNMT activity in endothelial cells. Similarly, shRNA-mediated silencing based on three different RNA sequences resulted in profound down-regulation of mRNA for NNMT, supporting the effective silencing of NNMT. Using pharmacological and molecular approaches, we demonstrated that the inhibition of NNMT sensitized both HAEC and HMEC-1 cells to menadione-induced oxidative stress, decreasing cell viability. Similar results were obtained in the endothelial lines EA.hy926 where NNMT was silenced, thus confirming that the reduction in cell viability in the oxidative stress model, upon NNMT inhibition, was indeed NNMT related.

Previous studies in other cell types suggested that NNMT enhances cellular resistance to radiation in the context of cancer [58]. The ionizing radiation used in radiotherapy induces free radical production; the generated ROS reacts with DNA causing single- or double stranded-breaks, and NNMT was reported to be downregulated in a radiosensitive bladder carcinoma cell line [59]. Moreover, nicotinamide is known to be a radiation sensitizer and is used clinically, also acting as a PARP inhibitor; thus, the inhibition of NNMT resulting in accumulation of nicotinamide could result in the attenuation of efficient single-stranded DNA break repair [60,61]. Our results in endothelial cells agree with other reports in other cell types, suggesting a cytoprotective role of NNMT. In particular, our findings show that NNMT in the endothelium protected endothelial cells against oxidative stress, and NNMT inhibition had detrimental cell viability effects in the well-known model of oxidative stress injury induced by menadione [62,63]. Co-incubation of menadione > 20 μM and NNMT inhibitors up-regulated vWF-specific fluorescence confirming that NNMT displays also anti-inflammatory effect in oxidative stress-mediated endothelial inflammation (data not shown).

In previous works, the mechanisms of the beneficial role of NNMT were linked to bioenergetics, the SIRT-1-dependent pathway or other mechanisms [7,31,64]. Here, we verify a possible involvement of two of these mechanisms in endothelial cells. NNMT as a major enzymatic source of nicotinamide methylation may indeed affect the NAD+ pool, a process that is dependent on constant re-synthesis from endogenous nicotinamide. Downregulation or pharmacological inhibition of NNMT in mouse models of diet-induced obesity increased NAD+ content in adipocytes [15,65], whereas in the OVCAR-3 cancer cell line, the increased expression of NNMT resulted in decreased parameters of mitochondrial oxygen consumption (basal respiration, maximal respiration, ATP production), measured by the Seahorse assay [66]. On the other

hand, the expression of NNMT in SH-SY5Y human neuroblastoma cells, which have no endogenous expression of NNMT, significantly increased ATP synthesis [64]. Our results did not confirm any significant change in the bioenergetic parameters induced by prolonged pharmacological NNMT inhibition, suggesting that in endothelial cells, this enzyme does not affect mitochondrial function. Accordingly, we excluded a possibility that the decrease in cell viability in response to oxidative stress in the presence of NNMT inhibition was linked to a collapse of the bioenergetic balance of the cell. The cytoprotective effects of NNMT in the endothelium were also not associated with an altered endothelial proliferation profile as also excluded in the present work. These results underscored a distinct role of endothelial NNMT as compared to cancer cells [67]. In turn, NNMT inhibition in the endothelium led to the downregulation of nuclear SIRT1, associated with upregulation of nuclear pSIRT1 resulting in an increased pSIRT1/SIRT1 ratio as compared to the control, suggesting the involvement of nuclear SIRT-dependent pathways in the cytoprotective effects of NNMT in the endothelium in an oxidant stress-induced model. These results were confirmed by enhanced cellular damage after SIRT1 inhibition, which was reflected by increased p53 expression. The upregulation of p53 after inactivation of SIRT1 has been previously reported [68] and this mechanism has an indubitable effect on cell survival under oxidative stress conditions.

SIRT1 exerts vasoprotective activity, inhibits endothelial senescence and inflammation [69–71], and a decreased SIRT1 expression and activity is associated with the progression of endothelial dysfunction and senescence [72,73]. In our experimental setting, co-incubation of menadione > 20 µM and NNMT inhibitors up-regulated vWF-specific fluorescence confirming that NNMT displays also anti-inflammatory effect in oxidative stress-mediated endothelial inflammation (data not shown). Many of the beneficial effects of SIRT1 in stress responses, cell survival, senescence and metabolism [74] are mediated via histones' or other signalling proteins' deacetylation, including peroxisome proliferator-activated receptor-g coactivator-1a (PGC-1a), forkhead transcription factor O (FoxO), nuclear factor kB (NFkB), endothelial nitric oxide synthase (eNOS), notch1 intracellular domain (NICD), liver kinase B1 (LKB1) and tumour suppressor protein 53 (p53) [73,75–80]. On the other hand, the SIRT1 phosphorylation on Ser47 results in increased nuclear localization of SIRT1, that by the mechanism shown to be dependent on cyclin-dependent kinase 5 (CDK5)-mediated hyper-phosphorylation of SIRT1 at Ser47 contributed to senescence and atherosclerosis [81]. In turn, the mammalian target of rapamycin (mTOR)-dependent phosphorylation of Ser47 resulted in the inhibition of SIRT1 deacetylase activity [82]. We did not investigate here whether the effects of NNMT inhibition on phosphorylation of SIRT1 at Ser47 were mediated by CDK5 or mTOR. We also did not analyze whether the NNMT inhibition affected the nuclear SIRT1 pathway by nicotinamide accumulation or downregulation of MNA. Previously, MNA was shown to stabilize the activity of SIRT1 in the liver [7]. On the other hand, increasing intracellular levels of nicotinamide may lead to the inhibition of SIRT1 [83–85]. Further studies are necessary to elucidate the mechanisms explaining the NNMT/SIRT1 interacting pathways.

Vasoprotection afforded by endothelial SIRT1 in vivo may be mediated by the intercellular cross-talk of SIRT1 in endothelium with soluble guanylyl cyclase in smooth muscle [86,87]. Clearly, further studies are necessary to elucidate the mechanisms underlying the vasoprotective NNMT pathway and its link with SIRT1-mediated pathways also in an *in vivo* setting.

Nevertheless, our results suggest that NNMT/SIRT1 interaction in the endothelium exerts a protective effect against oxidative stress, confirming the cytoprotective role of NNMT demonstrated in other models [88]. An important and surprising finding was that the nucleus was the major co-localization site of SIRT1 and NNMT, pointing to their important role in stress response. In fact, an interesting finding of this work was the observation that menadione-induced oxidative stress resulted in increased NNMT expression, suggesting that NNMT could act as a rescue enzyme upregulated in response to oxidant stress or possibly other stress conditions.

5. Conclusions

In the present study, we demonstrated (to our knowledge for the first time) that NNMT is present in the endothelium and exerts a protective role against oxidative stress that could be ascribed to the activity of SIRT1. Further studies are required to provide a deeper insight into the mechanism and disclose which downstream pathways are related to nuclear SIRT1 and pSIRT and which are affected by NNMT inhibition. This knowledge will enable our findings to be used to develop a novel therapeutic strategy against oxidative stress in endothelial cells.

Acknowledgements

Declarations of interest: none

FIGURE LEGEND

Figure 1. **NNMT and AOX1 expression levels**. Protein lysates obtained from endothelial HAEC, HMEC-1, HUVEC, hLMVEC, EA.hy926, MDA-MB-231 and MCF-7 cells were analyzed by Western blot to evaluate NNMT (Fig. 1A) and AOX1 (Fig. 1B) expression levels.

Figure 2. NNMT activity and MNA production. HMEC-1 cells (A), HAEC cells (C) and aliquots of mice liver (20 mg, D) were incubated in Krebs buffer with nicotinamide 100 μM, SAM 10 μM and 5MQ or JBSF-88 for 2 h. HMEC-1 cells (B) were incubated for 24h in full medium with 5MQ or JBSF-88 and nicotinamide 100 μM, SAM 10 μM.

Figure 3. **Effect of NNMT inhibition on cell viability after menadione-induced injury.** HAECs (A, B) and HMEC-1 (C, D) were incubated for 24 h with different concentrations of menadione together with 5MQ or JBSF-88, and cell viability was assessed by counting surviving cells through the automatic CQ-1 station and subsequent Columbus software analysis. Values are reported as mean ± standard deviation (n = 6, * p < 0.05, ** p < 0.01).

Figure 4. **Effect of NNMT knockdown on cell viability after menadione-induced injury.** EA.hy926 cells were transfected with 3 shRNA plasmids against NNMT (1–330, 1-448 and 1–711) or with empty plasmid vector (pLKO.1∅) or with transfection reagent only (CTRL). NNMT expression levels were evaluated by real-time PCR (A) and western blot (B). NNMT-silenced lines were incubated for 24 h with different concentrations of menadione, and cell viability was assessed by counting surviving cells through the automatic CQ-1 station and subsequent Columbus software analysis (n = 3, * p < 0.05).

Figure 5. **Effects of NNMT-inhibition on Yo-Pro1 positive staining in HAECs subjected or not to menadione-induced injury.** HAEC cells were incubated for 24 h with various concentrations of menadione together with JBSF-88 3 μM or 30 μM (A) or for 72 h with NNMT inhibitors only (B, C). Yo-Pro1 iodide-positive cells were detected by live imaging through the automatic CQ-1 station and subsequent Columbus software analysis (n = 6, * p < 0.05, ** p < 0.01, *** p < 0.001).

Figure 6. **Effect of NNMT inhibition on mitochondrial function and cell proliferation.** Key parameters of mitochondrial function were analyzed on HAECs using a Seahorse XF96 Cell Analyzer as described in the methods. (A) basal respiration, (B) proton leak, (C) maximal respiration, (D) ATP production.
The rate of cell proliferation of HAECs (E) and HMEC-1 (F) incubated with NNMT inhibitors was measured in real-time on the ECIS instrument by monitoring the resistance parameter at 4 kHz up to 150 h.

Figure 7. **Results of SIRT1 and phospho(Ser47)SIRT1 immunostaining in nucleus after 72 h incubation with NNMT inhibitor JBSF-88.** Diagrams showing SIRT1- and phospho(Ser47)SIRT1-specific fluorescence in the nuclear area after 72 h incubation with 5MQ (A) and JBSF-88 (B); representative images showing SIRT1 and phospho(Ser47)SIRT1 expression in the nucleus after treatment with 5MQ (C) or JBSF-88 (D); representative images of immunostained phospho(Ser47)SIRT1 in the nuclear area (C); n = 6, **p≤0.01, *** p≤0.001.

Figure 8. **NNMT, SIRT1 and pSIRT1 expression levels in menadione-treated HAECs.** HAECs were incubated for 48 h with increasing concentrations of menadione (A), and the expression of NNMT (B, E), SIRT1 (C, E) and pSIRT1 (D, E) was assessed by immunocytochemistry using the automatic CQ-1 station and subsequent Columbus software analysis (n = 3, * p < 0.05, ** p < 0.01, *** p < 0.001).

References

[1]   S. Aksoy, C.L. Szumlanski, R.M. Weinshilboum, Human liver nicotinamide N-methyltransferase cDNA cloning, expression, and biochemical characterization, J. Biol. Chem., 269 (1994).

[2]   Y. Peng, D. Sartini, V. Pozzi, D. Wilk, M. Emanuelli, V.C. Yee, Structural basis of substrate recognition in human nicotinamide N-methyltransferase, Biochemistry, 50 (2011) 7800–7808.

[3]   F. Li, Z. Chong, K. Maiese, Cell Life Versus Cell Longevity: The Mysteries Surrounding the NAD+ Precursor Nicotinamide, Curr. Med. Chem., (2006).

[4]   R.H. Houtkooper, C. Cantó, R.J. Wanders, J. Auwerx, The secret life of NAD+: An old metabolite controlling new metabolic signaling pathways, Endocr. Rev., (2010).

[5]   M. Riederer, W. Erwa, R. Zimmermann, S. Frank, R. Zechner, Adipose tissue as a source of nicotinamide N-methyltransferase and homocysteine, Atherosclerosis, 204 (2009) 412–417.

[6]   K. Ström, D. Morales-Alamo, F. Ottosson, A. Edlund, L. Hjort, S.W. Jörgensen, P. Almgren, Y. Zhou, M. Martin-Rincon, C. Ekman, A. Pérez-López, O. Ekström, I. Perez-Suarez, M. Mattiasson, P. De Pablos-Velasco, N. Oskolkov, E. Ahlqvist, N. Wierup, L. Eliasson, A. Vaag, et al., N1-methylnicotinamide is a signalling molecule produced in skeletal muscle coordinating energy metabolism, Sci. Rep., (2018).

[7]   S. Hong, J.M. Moreno-Navarrete, X. Wei, Y. Kikukawa, I. Tzameli, D. Prasad, Y. Lee, J.M. Asara, J.M. Fernandez-Real, E. Maratos-Flier, P. Pissios, Nicotinamide N-methyltransferase regulates hepatic nutrient metabolism through Sirt1 protein stabilization, Nat. Med., 21 (2015) 887–894.

[8]   T. Koppe, B. Patchen, A. Cheng, M. Bhasin, C. Vulpe, R.E. Schwartz, J.M. Moreno-Navarrete, J.M. Fernandez-Real, P. Pissios, P.G. Fraenkel, Nicotinamide N-methyltransferase expression decreases in iron overload, exacerbating toxicity in mouse hepatocytes, Hepatol. Commun., (2017).

[9]   M. Komatsu, T. Kanda, H. Urai, A. Kurokochi, R. Kitahama, S. Shigaki, T. Ono, H. Yukioka, K. Hasegawa, H. Tokuyama, H. Kawabe, S. Wakino, H. Itoh, NNMT activation can contribute to the development of fatty liver disease by modulating the NAD+metabolism, Sci. Rep., 8 (2018).

[10]   M. Liu, A. He, J. Chu, C. Chen, S. Zhang, Y. He, W. Tao, M. Lu, M. Hua, W. Ju, Z. Fang, Serum N1-methylnicotinamide is Associated with Left Ventricular Systolic Dysfunction in Chinese, Sci. Rep., 8 (2018).

[11]   M. Liu, L. Li, J. Chu, B. Zhu, Q. Zhang, X. Yin, W. Jiang, G. Dai, W. Ju, Z. Wang, Q. Yang, Z. Fang, Serum N1-methylnicotinamide is associated with obesity and diabetes in Chinese, J. Clin. Endocrinol. Metab., (2015).

[12]   A. Kannt, S. Rajagopal, S.V. Kadnur, J. Suresh, R.K. Bhamidipati, S. Swaminathan, M.S. Hallur, R. Kristam, R. Elvert, J. Czech, A. Pfenninger, C. Rudolph, H. Schreuder, D.V. Chandrasekar, V.S. Mane, S. Birudukota, S. Shaik, B.R. Zope, R.R. Burri, N.N. Anand, et al., A small molecule inhibitor of Nicotinamide N-methyltransferase for the treatment of metabolic disorders, Sci. Rep., 8 (2018).

[13]   H. Neelakantan, V. Vance, M.D. Wetzel, H.Y.L. Wang, S.F. McHardy, C.C. Finnerty, J.D. Hommel, S.J. Watowich, Selective and membrane-permeable small molecule inhibitors of nicotinamide N-methyltransferase reverse high fat diet-induced obesity in mice, Biochem. Pharmacol., 147 (2018) 141–152.

[14]   A. Kannt, A. Pfenninger, L. Teichert, A. Tonjes, A. Dietrich, M. Schon, N. Kloting, M. Bluher, Association of nicotinamide-N-methyltransferase mRNA expression in human adipose tissue and the plasma concentration of its product, 1-methylnicotinamide, with insulin resistance, Diabetologia, (2015).

[15]   D. Kraus, Q. Yang, D. Kong, A.S. Banks, L. Zhang, J.T. Rodgers, E. Pirinen, T.C. Pulinilkunnil, F. Gong, Y.C. Wang, Y. Cen, A.A. Sauve, J.M. Asara, O.D. Peroni, B.P. Monia, S. Bhanot, L. Alhonen, P. Puigserver, B.B. Kahn, Nicotinamide N-methyltransferase knockdown protects against diet-induced obesity, Nature, 508 (2014) 258–262.

[16]   R. Seta, M. Mascitti, R. Campagna, D. Sartini, S. Fumarola, A. Santarelli, M. Giuliani, M. Cecati, L. Lo Muzio, M. Emanuelli, Overexpression of nicotinamide N-methyltransferase in HSC-2 OSCC cell line: effect on apoptosis and cell proliferation, Clin. Oral Investig., (2018) 1–10.

[17]   J. Xu, F. Moatamed, J.S. Caldwell, J.R. Walker, Z. Kraiem, K. Taki, G.A. Brent, J.M. Hershman, Enhanced Expression of Nicotinamide N-Methyltransferase in Human Papillary Thyroid Carcinoma Cells, J. Clin. Endocrinol. Metab., 88 (2003) 4990–4996.

[18]   M. Tomida, I. Mikami, S. Takeuchi, H. Nishimura, H. Akiyama, Serum levels of nicotinamide N-methyltransferase in patients with lung cancer, J. Cancer Res. Clin. Oncol., 135 (2009) 1223–1229.

[19]   B.H. Lim, B.I. Cho, N.K. Yu, W.K. Jae, S.T. Park, C.W. Lee, Overexpression of nicotinamide N-methyltransferase in gastric cancer tissues and its potential post-translational modification, Exp. Mol. Med., 38 (2006) 455–465.

[20]   C.D. Rogers, N. Fukushima, N. Sato, C. Shi, N. Prasad, S.R. Hustinx, H. Matsubayashi, M. Canto, J.R. Eshleman, R.H. Hruban, M. Goggins, Differentiating pancreatic lesions by microarray and QPCR analysis of pancreatic juice RNAs, Cancer Biol. Ther., 5 (2006) 1383–1389.

[21]   M. Roessler, W. Rollinger, S. Palme, M.-L. Hagmann, P. Berndt, A.M. Engel, B. Schneidinger, M. Pfeffer, H. Andres, J. Karl, H. Bodenmüller, J. Rüschoff, T. Henkel, G. Rohr, S. Rossol, W. Rösch, H. Langen, W. Zolg, M. Tacke, Identification of nicotinamide N-methyltransferase as a novel serum tumor marker for colorectal cancer, Clin. Cancer Res., 11 (2005) 6550–7.

[22]   D. Sartini, G. Muzzonigro, G. Milanese, F. Pierella, V. Rossi, M. Emanuelli, Identification of nicotinamide N-methyltransferase as a novel tumor marker for renal clear cell carcinoma, J. Urol., 176 (2006) 2248–54.

[23]   R. Campagna, M. Cecati, V. Pozzi, V. Fumarola, Stefania Pompei, M. Giulio, A.B. Galosi, D. Sartini, M. Emanuelli, Involvement of transforming growth factor beta 1 in the transcriptional regulation of nicotinamide N-methyltransferase in clear cell renal cell carcinoma, Cell Mol Biol, 64 (2018) 51–55.

[24]   V. Pozzi, G. Di Ruscio, D. Sartini, R. Campagna, R. Seta, P. Fulvi, A. Vici, G. Milanese, G. Brandoni, A.B. Galosi, R. Montironi, M. Cecati, M. Emanuelli, Clinical performance and utility of a NNMT-based urine test for bladder cancer, Int. J. Biol. Markers, 33 (2018) 94–101.

[25]   A. Tsuchiya, M. Sakamoto, J. Yasuda, M. Chuma, T. Ohta, M. Ohki, T. Yasugi, Y. Taketani, S. Hirohashi, Expression Profiling in Ovarian Clear Cell Carcinoma: Identification of Hepatocyte Nuclear Factor-1β as a Molecular Marker and a Possible Molecular Target for Therapy of Ovarian Clear Cell Carcinoma, Am. J. Pathol., (2003).

[26]   G. Ganzetti, D. Sartini, A. Campanati, C. Rubini, E. Molinelli, V. Brisigotti, M. Cecati, V. Pozzi, R. Campagna, A. Offidani, M. Emanuelli, Nicotinamide N-methyltransferase: potential involvement in cutaneous malignant melanoma, Melanoma Res, 28 (2018) 82–88.

[27]   M. Mascitti, A. Santarelli, D. Sartini, C. Rubini, G. Colella, E. Salvolini, G. Ganzetti, A. Offidani, M. Emanuelli, Analysis of nicotinamide N-methyltransferase in oral malignant melanoma and potential prognostic significance, Melanoma Res., (2019).

[28]   T. Yu, Y.T. Wang, P. Chen, Y.H. Li, Y.X. Chen, H. Zeng, A.M. Yu, M. Huang, H.C. Bi, Effects of nicotinamide n-methyltransferase on PANC-1 cells proliferation, metastatic potential and survival under metabolic stress, Cell. Physiol. Biochem., 35 (2015) 710–721.

[29]   S.W. Tang, T.C. Yang, W.C. Lin, W.H. Chang, C.C. Wang, M.K. Lai, J.Y. Lin, Nicotinamide N-methyltransferase induces cellular invasion through activating matrix metalloproteinase-2 expression in clear cell renal cell carcinoma cells, Carcinogenesis, 32 (2011) 138–145.

[30]   V. Pozzi, D. Sartini, S. Morganti, R. Giuliante, G. Di Ruscio, A. Santarelli, R. Rocchetti, C. Rubini, M. Tomasetti, G. Giannatempo, F. Orlando, M. Provinciali, L. Lo Muzio, M. Emanuelli, RNA-Mediated Gene Silencing of Nicotinamide N-Methyltransferase Is Associated with Decreased Tumorigenicity in Human Oral Carcinoma Cells, PLoS One, 8 (2013).

[31] O.A. Ulanovskaya, A.M. Zuhl, B.F. Cravatt, NNMT promotes epigenetic remodeling in cancer by creating a metabolic methylation sink, Nat. Chem. Biol., 9 (2013) 300–306.

[32] R.B. Parsons, S.W. Smith, R.H. Waring, A.C. Williams, D.B. Ramsden, High expression of nicotinamide N-methyltransferase in patients with idiopathic Parkinson's disease, Neurosci. Lett., 342 (2003) 13–16.

[33] R.B. Parsons, M.L. Smith, A.C. Williams, R.H. Waring, D.B. Ramsden, Expression of nicotinamide N-methyltransferase (EC 2111) in the Parkinsonian brain, J. Neuropathol. Exp. Neurol., 61 (2002) 111–124.

[34] R. Giuliante, D. Sartini, T. Bacchetti, R. Rocchetti, I. Klöting, C. Polidori, G. Ferretti, M. Emanuelli, Potential involvement of nicotinamide N-methyltransferase in the pathogenesis of metabolic syndrome, Metab. Syndr. Relat. Disord., 13 (2015) 165–70.

[35] R. Debigaré, F. Maltais, C.H. Côté, A. Michaud, M.A. Caron, M. Mofarrahi, P. LeBlanc, S.N.A. Hussain, Profiling of mRNA expression in quadriceps of patients with COPD and muscle wasting, COPD J. Chronic Obstr. Pulm. Dis., 5 (2008) 75–84.

[36] A. Fedorowicz, Ł. Mateuszuk, G. Kopec, T. Skórka, B. Kutryb-Zajac, A. Zakrzewska, M. Walczak, A. Jakubowski, M. Łomnicka, E. Słomińska, S. Chlopicki, Activation of the nicotinamide N-methyltransferase (NNMT)-1-methylnicotinamide (MNA) pathway in pulmonary hypertension, Respir. Res., 17 (2016).

[37] Ł. Mateuszuk, T.I. Khomich, E. Słomińska, M. Gajda, L. Wójcik, M. Łomnicka, P. Gwóźdź, S. Chłopicki, Activation of nicotinamide N-methyltrasferase and increased formation of 1-methylnicotinamide (MNA) in atherosclerosis, in: Pharmacol. Reports, 2009: pp. 76–85.

[38] M.C. Bergagnini-Kolev, M.F. Hebert, T.R. Easterling, Y.S. Lin, Pregnancy increases the renal secretion of N1-methylnicotinamide, an endogenous probe for renal cation transporters, in patients prescribed metformin, Drug Metab. Dispos., (2017).

[39] S. Chlopicki, J. Swies, A. Mogielnicki, W. Buczko, M. Bartus, M. Lomnicka, J. Adamus, J. Gebicki, 1-Methylnicotinamide (MNA), a primary metabolite of nicotinamide, exerts anti-thrombotic activity mediated by a cyclooxygenase-2/prostacyclin pathway, Br. J. Pharmacol., 152 (2007) 230–239.

[40] K. Bryniarski, R. Biedron, A. Jakubowski, S. Chlopicki, J. Marcinkiewicz, Anti-inflammatory effect of 1-methylnicotinamide in contact hypersensitivity to oxazolone in mice; involvement of prostacyclin, Eur. J. Pharmacol., 578 (2008) 332–338.

[41] T. Brzozowski, P.C. Konturek, S. Chlopicki, Z. Sliwowski, M. Pawlik, A. Ptak-Belowska, S. Kwiecień, D. Drozdowicz, R. Pajdo, E. Slonimska, S.J. Konturek, W.W. Pawlik, Therapeutic potential of 1-methylnicotinamide against acute gastric lesions induced by stress: Role of endogenous

prostacyclin and sensory nerves, J. Pharmacol. Exp. Ther., (2008).

[42] M. Sternak, A. Jakubowski, E. Czarnowska, E.M. Slominska, R.T. Smolenski, M. Szafarz, M. Walczak, B. Sitek, T. Wojcik, A. Jasztal, K. Kaminski, S. Chlopicki, Differential involvement of IL-6 in the early and late phase of 1-methylnicotinamide (MNA) release in Concanavalin A-induced hepatitis, Int. Immunopharmacol., (2015).

[43] A. Jakubowski, M. Sternak, K. Jablonski, M. Ciszek-Lenda, J. Marcinkiewicz, S. Chlopicki, 1-Methylnicotinamide protects against liver injury induced by concanavalin A via a prostacyclin-dependent mechanism: A possible involvement of IL-4 and TNF-α, Int. Immunopharmacol., (2016).

[44] R. hao Mu, Y. zhi Tan, L. li Fu, M. Nazmul Islam, M. Hu, H. Hong, S. su Tang, 1-Methylnicotinamide attenuates lipopolysaccharide-induced cognitive deficits via targeting neuroinflammation and neuronal apoptosis, Int. Immunopharmacol., (2019).

[45] L. Fu, C. Liu, L. Chen, Y. Lv, G. Meng, M. Hu, Y. Long, H. Hong, S. Tang, Protective Effects of 1-Methylnicotinamide on Aβ1–42-Induced Cognitive Deficits, Neuroinflammation and Apoptosis in Mice, J. Neuroimmune Pharmacol., (2019).

[46] A. Blazejczyk, M. Switalska, S. Chlopicki, A. Marcinek, J. Gebicki, M. Nowak, A. Nasulewicz-Goldeman, J. Wietrzyk, 1-methylnicotinamide and its structural analog 1,4-dimethylpyridine for the prevention of cancer metastasis, J. Exp. Clin. Cancer Res., (2016).

[47] A. Denslow, M. Switalska, M. Nowak, M. Maciejewska, S. Chlopicki, A. Marcinek, J. Gebicki, J. Wietrzyk, The effects of 1,4-Dimethylpyridine in metastatic prostate cancer in mice, BMC Cancer, (2017).

[48] L. Mateuszuk, A. Jasztal, E. Maslak, M. Gasior-Glogowska, M. Baranska, B. Sitek, R. Kostogrys, A. Zakrzewska, A. Kij, M. Walczak, S. Chlopicki, Antiatherosclerotic effects of 1-methylnicotinamide in apolipoprotein e/low-density lipoprotein receptor-deficient mice: A comparison with nicotinic acid, J. Pharmacol. Exp. Ther., (2016).

[49] A. Bar, M. Olkowicz, U. Tyrankiewicz, E. Kus, K. Jasinski, R.T. Smolenski, T. Skorka, S. Chlopicki, Functional and biochemical endothelial profiling in vivo in a murine model of endothelial dysfunction; comparison of effects of 1-methylnicotinamide and angiotensin-converting enzyme inhibitor, Front. Pharmacol., (2017).

[50] N. Hamilton, G. SJA, M. Kiczun, J. Morphy, B. Sherborne, P. Littlewood, A. Brown, C. Kingsbury, M. Ohlmeyer, K. Ho, S. Kultgen, No Title, Pharmacop. Drug Discov. Inc., (2007) US 2007/149577, A1.

[51] R. Benesh, M. Blanco-Pillado, No Title, Eli Lilly Co., (2005) WO 2005/61442 A1.

[52] H. Neelakantan, H.Y. Wang, V. Vance, J.D. Hommel, S.F. McHardy, S.J. Watowich, Structure-

Activity Relationship for Small Molecule Inhibitors of Nicotinamide N-Methyltransferase, J. Med. Chem., (2017).

[53] J. Zhang, Y. Wang, G. Li, H. Yu, X. Xie, Down-regulation of nicotinamide N-methyltransferase induces apoptosis in human breast cancer cells via the mitochondria-mediated pathway, PLoS One, 9 (2014).

[54] K. Maeda, T. Ohno, S. Igarashi, T. Yoshimura, K. Yamashiro, M. Sakai, Aldehyde oxidase 1 gene is regulated by Nrf2 pathway, Gene, (2012).

[55] M. Bartuś, M. Łomnicka, R.B. Kostogrys, P. Kaźmierczak, C. Watala, E.M. Słominska, R.T. Smoleński, P.M. Pisulewski, J. Adamus, J. Gebicki, S. Chlopicki, 1-Methylnicotinamide (MNA) prevents endothelial dysfunction in hypertriglyceridemic and diabetic rats, in: Pharmacol. Reports, 2008: pp. 127–138.

[56] M. Sternak, T.I. Khomich, A. Jakubowski, M. Szafarz, W. Szczepański, M. Białas, M. Stojak, J. Szymura-Oleksiak, S. Chłopicki, Nicotinamide n-methyltransferase (nnmt) and 1-methylnicotinamide (mna) in experimental hepatitis induced by concanavalin a in the mouse, Pharmacol. Reports, 62 (2010) 483–493.

[57] M. Nayor, R. V. Shah, P.E. Miller, J.B. Blodgett, M. Tanguay, A.R. Pico, V.L. Murthy, R. Malhotra, N.E. Houstis, A. Deik, K.A. Pierce, K. Bullock, L. Dailey, R.S. Velagaleti, S.A. Moore, J.E. Ho, A.L. Baggish, C.B. Clish, M.G. Larson, R.S. Vasan, et al., Metabolic Architecture of Acute Exercise Response in Middle-Aged Adults in the Community, Circulation, (2020).

[58] F.P. D'Andrea, A. Safwat, M. Kassem, L. Gautier, J. Overgaard, M.R. Horsman, Cancer stem cell overexpression of nicotinamide N-methyltransferase enhances cellular radiation resistance, Radiother. Oncol., 99 (2011) 373–378.

[59] H.S. Kassem, V. Sangar, R. Cowan, N. Clarke, G.P. Margison, A potential role of heat shock proteins and nicotinamide N-methyl transferase in predicting response to radiation in bladder cancer, Int. J. Cancer, 101 (2002) 454–460.

[60] M.R. Horsman, D.W. Siemann, D.J. Chaplin, J. Overgaard, Nicotinamide as a radiosensitizer in tumours and normal tissues: The importance of drug dose and timing, Radiother. Oncol., (1997).

[61] P.J. Hoskin, A.M. Rojas, M.I. Saunders, S.M. Bentzen, K.J. Motohashi, Carbogen and nicotinamide in locally advanced bladder cancer: Early results of a phase-III randomized trial, Radiother. Oncol., (2009).

[62] W. Kossenjans, Z. Rymaszewski, J. Barankiewicz, A. Bobst, M. Ashraf, Menadione-Induced Oxidative Stress in Bovine Heart Microvascular Endothelial Cells, Microcirculation, (1996).

[63] W.C. McAmis, R.C. Schaeffer, J.W. Baynes, M.B. Wolf, Menadione causes endothelial barrier
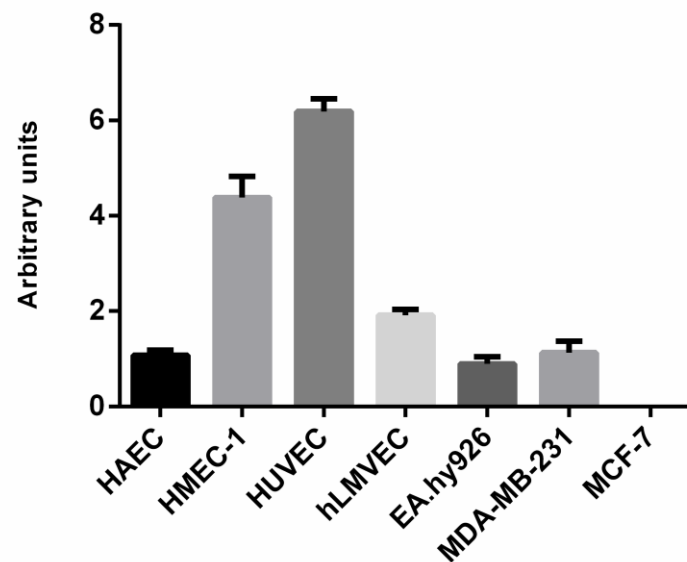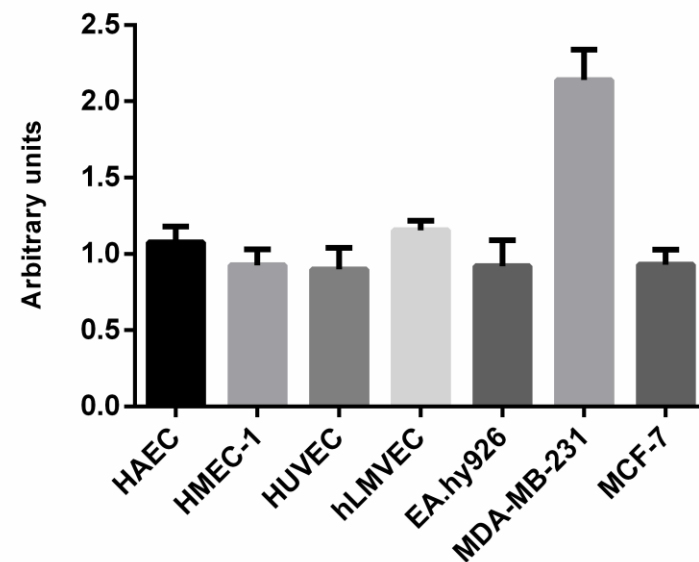
failure by a direct effect on intracellular thiols, independent of reactive oxidant production, Biochim. Biophys. Acta - Mol. Cell Res., (2003).

[64]   K.Y. Liu, R.J. Mistry, C.A. Aguirre, E.S. Fasouli, M.G. Thomas, F. Klamt, D.B. Ramsden, R.B. Parsons, Nicotinamide N-methyltransferase increases complex i activity in SH-SY5Y cells via sirtuin 3, Biochem. Biophys. Res. Commun., 467 (2015) 491–496.

[65]   H. Neelakantan, C.R. Brightwell, T.G. Graber, R. Maroto, H.Y.L. Wang, S.F. McHardy, J. Papaconstantinou, C.S. Fry, S.J. Watowich, Small molecule nicotinamide N-methyltransferase inhibitor activates senescent muscle stem cells and improves regenerative capacity of aged skeletal muscle, Biochem. Pharmacol., (2019).

[66]   A. Kanakkanthara, K. Kurmi, T.L. Ekstrom, X. Hou, E.R. Purfeerst, E.P. Heinzen, C. Correia, C.J. Huntoon, D. O'Brien, A.E. Wahner Hendrickson, S.C. Dowdy, H. Li, A.L. Oberg, T. Hitosugi, S.H. Kaufmann, S.J. Weroha, L.M. Karnitz, BRCA1 deficiency upregulates NNMT, which reprograms metabolism and sensitizes ovarian cancer cells to mitochondrial metabolic targeting agents, Cancer Res., (2019).

[67]   V. Pozzi, M. Mazzotta, L. Lo Muzio, D. Sartini, A. Santarelli, E. Renzi, R. Rocchetti, M. Tomasetti, D. Ciavarella, M. Emanuelli, Inhibiting proliferation in KB cancer cells by RNA interference-mediated knockdown of nicotinamide N-methyltransferase expression, Int. J. Immunopathol. Pharmacol., 24 (2011) 69–77.

[68]   L. Hongyan, R. Wang, Blocking SIRT1 inhibits cell proliferation and promotes aging through the PI3K/AKT pathway, Life Sci, 190 (2017) 84–90.

[69]   S. Stein, C.M. Matter, Protective roles of SIRT1 in atherosclerosis, Cell Cycle, (2011).

[70]   H. Ota, M. Eto, S. Ogawa, K. Iijima, M. Akishita, Y. Ouchi, Sirt1/eNOS axis as a potential target against vascular senescence, dysfunction and atherosclerosis, J. Atheroscler. Thromb., (2010).

[71]   V. Guarani, M. Potente, SIRT1-a metabolic sensor that controls blood vessel growth, Curr. Opin. Pharmacol., (2010).

[72]   M. Orimo, T. Minamino, H. Miyauchi, K. Tateno, S. Okada, I. Komuro, Protective role of SIRT1 in diabetic vascular dysfunction, Arterioscler. Thromb. Vasc. Biol., (2009).

[73]   Y. Zu, L. Liu, M.Y.K. Lee, C. Xu, Y. Liang, R.Y. Man, P.M. Vanhoutte, Y. Wang, SIRT1 promotes proliferation and prevents senescence through targeting LKB1 in primary porcine aortic endothelial cells, Circ. Res., (2010).

[74]   Y. Guo, A. Xu, Y. Wang, SIRT1 in Endothelial Cells as a Novel Target for the Prevention of Early Vascular Aging, J. Cardiovasc. Pharmacol., (2016).
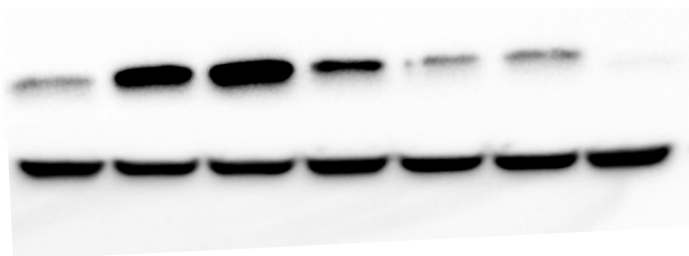
[75] S. Xiong, G. Salazar, N. Patrushev, M. Ma, F. Forouzandeh, L. Hilenski, R.W. Alexander, Peroxisome proliferator-activated receptor γ coactivator-1α is a central negative regulator of vascular senescence, Arterioscler. Thromb. Vasc. Biol., (2013).

[76] K.N. Papanicolaou, Y. Izumiya, K. Walsh, Forkhead transcription factors and cardiovascular biology, Circ. Res., (2008).

[77] Z. Liu, C. Jiang, J. Zhang, B. Liu, Q. Du, Resveratrol inhibits inflammation and ameliorates insulin resistant endothelial dysfunction via regulation of AMP-activated protein kinase and sirtuin 1 activities, J. Diabetes, (2016).

[78] N. Nualnim, J.N. Barnes, T. Tarumi, C.P. Renzi, H. Tanaka, Comparison of central artery elasticity in swimmers, runners, and the sedentary, Am. J. Cardiol., (2011).

[79] V. Guarani, G. Deflorian, C.A. Franco, M. Krüger, L.K. Phng, K. Bentley, L. Toussaint, F. Dequiedt, R. Mostoslavsky, M.H.H. Schmidt, B. Zimmermann, R.P. Brandes, M. Mione, C.H. Westphal, T. Braun, A.M. Zeiher, H. Gerhardt, S. Dimmeler, M. Potente, Acetylation-dependent regulation of endothelial Notch signalling by the SIRT1 deacetylase, Nature, (2011).

[80] J. Yi, J. Luo, SIRT1 and p53, effect on cancer, senescence and beyond, Biochim. Biophys. Acta - Proteins Proteomics, (2010).

[81] B. Bai, Y. Liang, C. Xu, M.Y.K. Lee, A. Xu, D. Wu, P.M. Vanhoutte, Y. Wang, Cyclin-dependent kinase 5-mediated hyperphosphorylation of sirtuin-1 contributes to the development of endothelial senescence and atherosclerosis, Circulation, (2012).

[82] M. Kitada, Y. Ogura, D. Koya, The protective role of Sirt1 in vascular tissue: Its relationship to vascular aging and atherosclerosis, Aging (Albany. NY)., (2016).

[83] A.A. Sauve, V.L. Schramm, Sir2 regulation by nicotinamide results from switching between base exchange and deacetylation chemistry, Biochemistry, (2003).

[84] M.D. Jackson, M.T. Schmidt, N.J. Oppenheimer, J.M. Denu, Mechanism of Nicotinamide Inhibition and Transglycosidation by Sir2 Histone/Protein Deacetylases, J. Biol. Chem., (2003).

[85] M.T. Borra, M.R. Langer, J.T. Slama, J.M. Denu, Substrate specificity and kinetic mechanism of the Sir2 family of NAD +-dependent histone/protein deacetylases, Biochemistry, (2004).

[86] Yumeng Guo, C. Xu, A.W.C. Man, B. Bai, C. Luo, Y. Huang, A. Xu, P.M. Vanhoutte, W. Yu, Endothelial SIRT1 prevents age-induced impairment of vasodilator responses by enhancing the expression and activity of soluble guanylyl cyclase in smooth muscle cells, Cardiovasc Res, 115 (2019) 678–690.

[87] R. Suades, F. Cosentino, Sirtuin 1/soluble guanylyl cyclase: a nitric oxide-independent pathway to

rescue ageing-induced vascular dysfunction, Cardiovasc Res, 115 (2019) 485–487.

[88]   K. Schmeisser, J. Mansfeld, D. Kuhlow, S. Weimer, S. Priebe, I. Heiland, M. Birringer, M. Groth, A. Segref, Y. Kanfi, N.L. Price, S. Schmeisser, S. Schuster, A.F.H. Pfeiffer, R. Guthke, M. Platzer, T. Hoppe, H.Y. Cohen, K. Zarse, D.A. Sinclair, et al., Role of sirtuins in lifespan regulation is linked to methylation of nicotinamide, Nat. Chem. Biol., 9 (2013) 693–700.

A NNMT protein expression

B AOX1 protein expression

Figure 1

Figure 2

Figure 3

Figure 4

A % of Yo-Pro1 positive cells (24h)

JBSF-88 3µM	-	+	-	-	+	-	-	+	-	-	+	-
JBSF-88 30µM	-	-	+	-	-	+	-	-	+	-	-	+
Men 0.5µM	-	-	-	+	+	+	-	-	-	-	-	-
Men 5µM	-	-	-	-	-	-	+	+	+	-	-	-
Men 10µM	-	-	-	-	-	-	-	-	-	+	+	+

B 5MQ (% of Yo-Pro1 positive cells)

C JBSF-88 (% of Yo-Pro1 positive cells)

Figure 5

Figure 6

Figure 7

A

nuclear pSIRT1/totSIRT1 ratio

B

nuclear pSIRT1/totSIRT1 ratio

C

D

Figure 8

A mean. no. of cells

B NNMT (cell)

C nuclear SIRT1

D nuclear p(Ser47)SIRT1

E NNMT   SIRT1   p(Ser47)SIRT1

A

cell number

[mean cell counts]

EX-527 10 μM	−	+	−	+	−	+	−	+	−	+
Menadione 10 μM	−	−	+	−	−	−	−	−	−	−
Menadione 20 μM	−	−	−	−	+	−	−	−	−	−
Menadione 30 μM	−	−	−	−	−	−	+	−	−	−
Menadione 40 μM	−	−	−	−	−	−	−	−	+	−

B

p53 (cell)

Cy3 fluoresc. [AU/cell counts]

EX-527 10 μM	−	+	−	+	−	+	−	+	−	+
Menadione 10 μM	−	−	+	−	−	−	−	−	−	−
Menadione 20 μM	−	−	−	−	+	−	−	−	−	−
Menadione 30 μM	−	−	−	−	−	−	+	−	−	−
Menadione 40 μM	−	−	−	−	−	−	−	−	+	−

C

Acetyl-p53 (cell)

AF647 fluoresc. [AU/cell counts]

EX-527 10 μM	−	+	−	+	−	+	−	+	−	+
Menadione 10 μM	−	−	+	−	−	−	−	−	−	−
Menadione 20 μM	−	−	−	−	+	−	−	−	−	−
Menadione 30 μM	−	−	−	−	−	−	+	−	−	−
Menadione 40 μM	−	−	−	−	−	−	−	−	+	−

Figure 9